metals

MDPI

Review

Effect of Hydrogen in Mixed Gases on the Mechanical Properties of Steels—Theoretical Background and Review of Test Results

Thorsten Michler [1,*], Christian Elsässer [1,2], Ken Wackermann [1] and Frank Schweizer [1]

[1] Fraunhofer Institute for Mechanics of Materials IWM, Woehlerstrasse 11, 79108 Freiburg, Germany; christian.elsaesser@iwm.fraunhofer.de (C.E.); ken.wackermann@iwm.fraunhofer.de (K.W.); frank.schweizer@iwm.fraunhofer.de (F.S.)

[2] Freiburg Materials Research Center (FMF), University of Freiburg, Stefan-Meier-Straße 21, 79104 Freiburg, Germany

* Correspondence: Thorsten.michler@iwm.fraunhofer.de

Abstract: This review summarizes the thermodynamics of hydrogen (H_2) in mixed gases of nitrogen (N_2), methane (CH_4) and natural gas, with a special focus on hydrogen fugacity. A compilation and interpretation of literature results for mechanical properties of steels as a function of hydrogen fugacity implies that test results obtained in gas mixtures and in pure hydrogen, both at the same fugacity, are equivalent. However, this needs to be verified experimentally. Among the test methods reviewed here, fatigue crack growth testing is the most sensitive method to measure hydrogen effects in pipeline steels followed by fracture toughness testing and tensile testing.

Keywords: hydrogen embrittlement; hydrogen pressure; fugacity; pipeline steels; gas mixtures

Citation: Michler, T.; Elsässer, C.; Wackermann, K.; Schweizer, F. Effect of Hydrogen in Mixed Gases on the Mechanical Properties of Steels—Theoretical Background and Review of Test Results. *Metals* **2021**, *11*, 1847. https://doi.org/10.3390/met11111847

Academic Editor: Heung Nam Han

Received: 18 October 2021
Accepted: 16 November 2021
Published: 17 November 2021

1. Introduction

Significant efforts are ongoing in the European Union and worldwide to defossilize private and industry sectors by reducing the emission of green house gases. In the energy sector, one important goal is to replace natural gas (NG) with hydrogen. This goal shall be reached stepwise by blending natural gas with increasing amounts of hydrogen (H_2). Worldwide, significant research activities are dedicated to investigate, whether the existing natural gas storage and transport infrastructure can be used for NG-H_2 blends with up to 30% of hydrogen or even for 100% hydrogen gas, see e.g., [1] for a German case study. The analysis of the material compatibility is one important aspect.

It is well established that the mechanical properties of most metallic alloys including steels deteriorate under the influence of hydrogen. This effect is often referred to as 'hydrogen embrittlement'. It is further known that the deterioration of mechanical properties of steels increases with increasing hydrogen concentration inside the steel, which increases with increasing hydrogen gas pressure, more precisely hydrogen fugacity [2]. The fugacity is often described as the activity of the real gas, i.e., the gas in states that are not well described by the ideal gas law. It has been found that the fugacity of pure hydrogen is different from the fugacity of hydrogen in gas mixtures [3] and that (small) additions of oxygen even mitigate hydrogen absorption into the steel [4,5].

Several publications report the effect of hydrogen in NG-H_2 gas blends upon the mechanical properties of steels, see e.g., [6,7]. In other publications, natural gas is replaced by methane (CH_4) [8] or nitrogen (N_2) [9] to exclude unwanted secondary effects originating from the complex chemical composition of natural gas. However, in most studies, the degradation of mechanical properties is plotted as a function of the volume fraction of H_2 added to NG at a given total gas pressure. To come to more general conclusions, such studies were reviewed, hydrogen fugacities were calculated, and results were compared to tests performed in pure hydrogen gas at comparable fugacities. It will be shown that

the hydrogen fugacity can be used as a single parameter to describe hydrogen effects on steels independent of testing these in a gas blend or in pure hydrogen, and that testing in gas blends is not necessary to assess hydrogen effects on materials used in NG-H_2 infrastructures.

2. Fugacity of Hydrogen in Gas Mixtures

The state of a real gas is described by the van der Waals equation of state (EOS) which takes into account finite sizes of molecules (co-volume parameter (b) and attractive interactions between molecules (molecular-attraction parameter (a) as follows:

$$\left(P + \frac{a}{V_m^2}\right)(V_m - b) = RT \tag{1}$$

with

- P: total pressure,
- R: universal gas constant, 8.314 J/(mol K),
- T: absolute temperature, K,
- V_m: molar volume.

The van der Waals EOS as well as other empirical relationships for non-ideal gases with two or more parameters, or virial expansions, are complicated to use for enginering applications because of non-linearities. For applications to hydrogen systems, the Abel-Noble EOS, which is a simplified one-parameter variant of the van der Waals EOS, setting the molecular-interaction parameter a to zero, provides a reasonably good description of hydrogen-gas data with a sufficient accuracy at relevant engineering conditions ($T > 223$ K and $p < 200$ MPa) [10].

The Estimation of the amount of hydrogen dissolved in the crystal lattice of a metal from a gas requires the knowledge of the fugacity. For hydrogen as a single-component gas, the Abel-Noble equation of state provides a sufficient prediction of it's real gas behaviour [10]. For a more general approach see e.g., [11].

The estimation of the hydrogen fugacity in gas mixtures of multiple components is presented in [3,12,13]. In the following the relevant equations are concisely summarized. For convenience, the same nomenclature as in [12] is used here. The hydrogen fugacity f_{HH} in a gas mixture of H_2 and another gas can be calculated as [12].

$$f_{HH} = x_{HH} P e^{\frac{Pb}{RT}} \tag{2}$$

with

- x_{HH}: molar fraction of H_2,
- P: total pressure of the gas mixture,
- b: co-volume constant of the gas mixture.

The molar fraction of hydrogen as well as the compressibility factors of H_2 and another gas in a mixture of two gases, (Z_{HH} and Z_{Gas}) can be calculated as [12]:

$$x_{HH} = \frac{\frac{p_{HH}}{Z_{HH}}}{\frac{p_{HH}}{Z_{HH}} + \frac{p_{Gas}}{Z_{Gas}}} \tag{3}$$

$$Z_{HH} = 1 + \frac{p_{HH} b_{HH}}{RT} \; and \; Z_{Gas} = 1 + \frac{p_{Gas} b_{Gas}}{RT} \tag{4}$$

with

- p_{HH}, p_{Gas}: partial pressures of H_2 and the other gas, respectively,
- b_{HH}, b_{Gas}: co-volume constants of H_2 and the other gas, respectively.

The co-volume constant of the gas mixture is defined as [13]:

$$b = x_{HH} b_{HH} + (1 - x_{HH}) b_{Gas} + \frac{x_{HH}(1 - x_{HH}) b_{HH} b_{Gas}}{2(b_{HH} + b_{Gas})} \quad (5)$$

Using this set of equations requires both b_{HH} and b_{Gas} for the calculation of f_{HH} in a gas mixture according Equation (2). Within the given temperature and pressure range for most engineering applications, the co-volume constant of hydrogen can be assumed as constant (b_{HH} = 15.84 cm^3/mol [10]) whereas the co-volume constant of the other gas (b_{Gas}) can be derived from Equation (4) as a function of pressure using experimentally measured compressibility factors.

It shall be emphasized here that the application of the Abel-Noble EOS is restricted to such gases as helium, neon or hydrogen where the kinetic interaction of the molecules can be neglected [13,14]. This is typically not the case for nitrogen (N_2), methane (CH_4) or natural gas (NG) [13,14]. However, it will be shown in the following that the error is acceptable using the Abel-Noble EOS to assess the fugacity of hydrogen in N_2-H_2 and CH_4-H_2 gas mixtures at relevant engineering conditions, e.g., room temperature and pressures up to 20 MPa.

Experimentally measured compressibility factors of N_2, CH_4 and NG are shown in Figure 1. The general trends of N_2, CH_4 and NG are similar. For N_2, Z drops slightly below unity with increasing pressure, reaches a minimum of about 0.994 at about 6 MPa and then strongly increases at pressures higher than 10 MPa to Z values significantly higher than unity. Since the decrease of Z below unity is very slight, it can fairly be assumed (at least for engineering purposes) that N_2 behaves like an ideal gas up to pressures of 10 MPa at room temperature. For CH_4 (and NG), Z drops significantly below unity with increasing pressure, reaches a minimum of about 0.8 at a pressure of about 16 MPa and then slightly increases with increasing pressure. $Z < 1$ means that the movement of the molecules in not hindered, i.e., the attractive forces dominate, which is captured by the molecular attraction parameter a in the Van der Waals equation (Equation (1)) and the co-volume parameter b can be neglected. On the other hand, $Z > 1$ means that repulsive forces between molecules dominate which is captured by the co-volume parameter b and the molecular attraction parameter a can be neglected. The results for N_2 and CH_4 from the different references appear very consistent (Figure 1a,b), while the results for NG (Figure 1c) scatter significantly presumably due to the different compositions of the natural gas qualities investigated in the individual studies. It can be seen that in terms of compressibility, natural gas is better represented by CH_4 than by N_2 because methane is the main constituent of natural gas, typically more than 80 vol%. However, both, the results for N_2 and CH_4 can be fitted by a polynomial function of the total pressure P as follows

$$Z = AP^5 + BP^4 + CP^3 + DP^2 + EP + F \quad (6)$$

with the coefficients given in Table 1.

Equation (6) and the fit coefficients from Table 1 can now be used to calculate Z_{Gas} for N_2 or CH_4, respectively. Now, the co-volume constant b_{Gas} can be calculated according to Equation (4). The results are shown in Figure 2 together with the corresponding compressibility factors.

Using the data from Figure 2, the co-volume constant of the respective gas mixture b (N_2-H_2 or CH_4-H_2) can be calculated according to Equation (5), and finally the fugacity of hydrogen in a gas mixture f_{HH} can be calculated according to Equation (2).

The error of this method can be assessed by comparing calculated compressibility factors of a gas mixture (Z_{mix}) using Equation (7) with experimentally measured compressibility factors.

$$Z_{mix} = 1 + \frac{Pb}{RT} \quad (7)$$

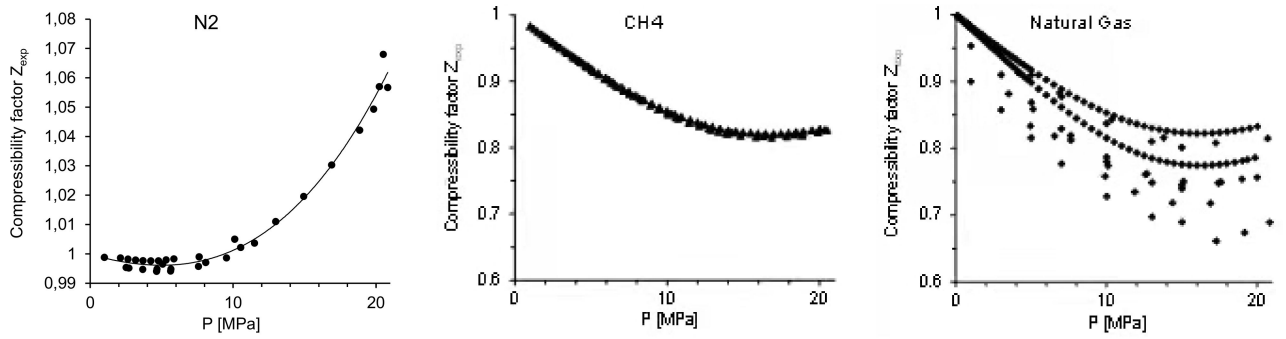

(**a**) (**b**) (**c**)

Figure 1. Experimental compressibility factors of (**a**) N_2 data from [15–17], (**b**) CH_4 data from [18–21] and (**c**) Natural Gas data from [20,22–25].

Table 1. Fit coefficients for the calculation of the compressibility factor according to Equation (6) and coefficient of determination (R^2) for N_2 and CH_4 according to Figure 1a,b.

Coefficient	N_2	CH_4
A, MPa^{-5}	0	−0.00000006
B, MPa^{-4}	0	0.00000200
C, MPa^{-3}	0.00000551	−0.00000243
D, MPa^{-2}	0.00009256	0.00012034
E, MPa^{-1}	−0.00133489	−0.01709066
F	0.99979310	1.00027004
R^2	0.98691955	0.99889577

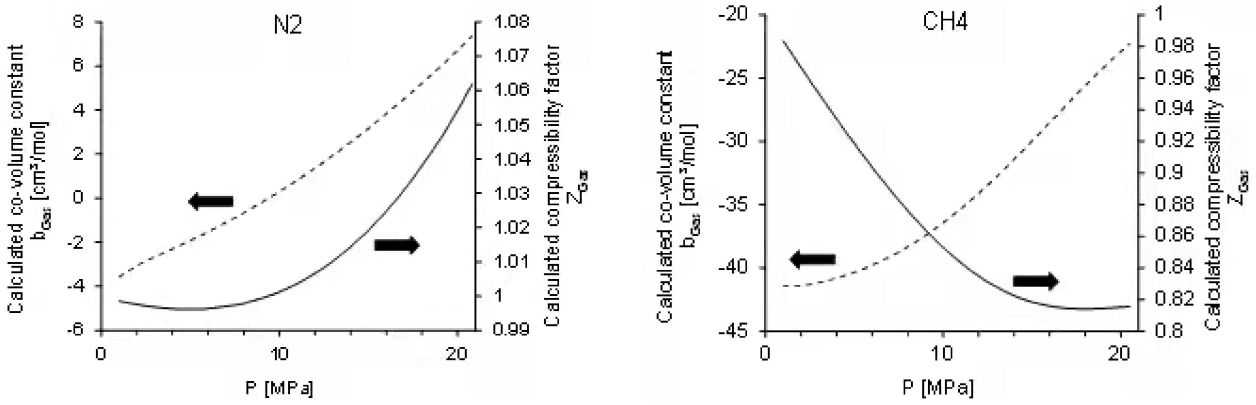

(**a**) (**b**)

Figure 2. Calculated co-volume constants and compressibility factors according to Equation (6) of (**a**) N_2, (**b**) CH_4.

Examples for a 75%N_2–25%H_2 and a 78%CH_4–22%H_2 gas mixture are shown in Figure 3. It can be seen that the absolute error between calculated and measured compressibility factors is less than 0.03 for the N_2-H_2 mixture and less than 0.08 for the CH_4-H_2 mixture at room temperature and the given pressure range. Such errors appear tolerable for engineering applications assessing hydrogen fugacities in mixed gases.

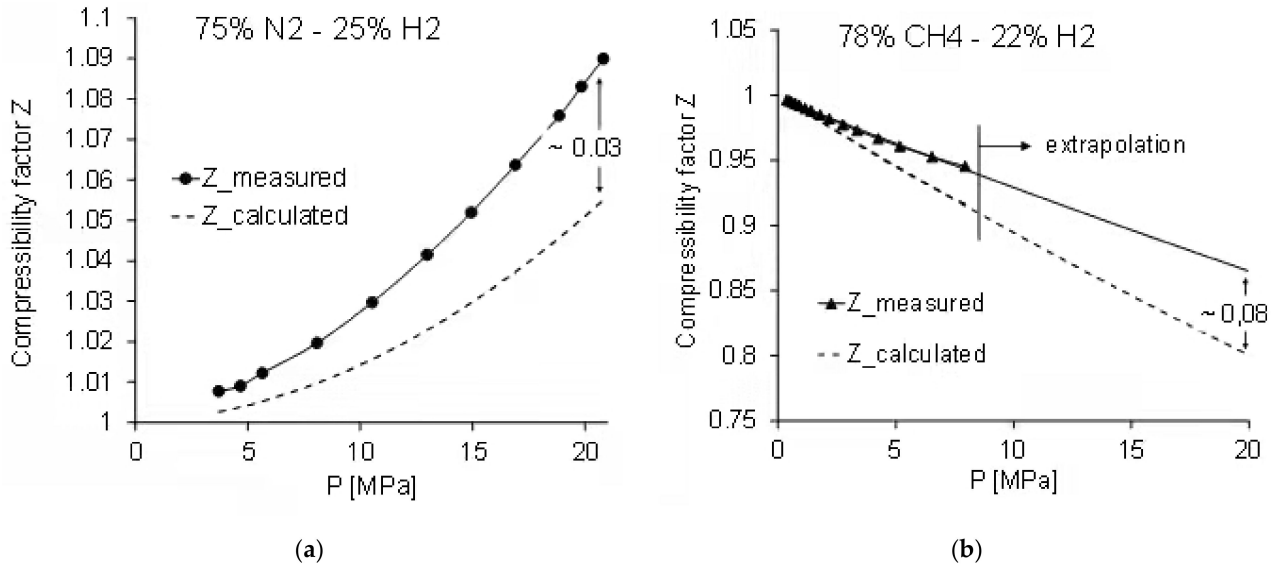

(**a**) (**b**)

Figure 3. Measured and calculated compressibility factors for (**a**) a 75%N_2–25% H_2 gas mixture [17] and (**b**) a 78% CH_4–22% H_2 gas mixture data from [21] as a function of total pressure *P*.

As an example, the evolution of f_{HH} as a function of p_{HH} in N_2-H_2 and CH_4-H_2 gas mixtures at a total pressure of 20 MPa is shown in Figure 4a. For N_2-H_2 gas mixtures, $f_{HH} \approx p_{HH}$ up to hydrogen partial pressures of about 10 MPa and $f_{HH} > p_{HH}$ for higher hydrogen partial pressures with f_{HH} up to about 22 MPa at p_{HH} = 20 MPa. For CH_4-H_2 gas mixtures, $f_{HH} < p_{HH}$ up to p_{HH} of about 15 MPa. The highest deviation is at p_{HH} = 9 MPa, where f_{HH} is calculated as low as about 7.2 MPa. In Figure 4b, the same data is plotted as a function of the hydrogen fugacity in pure hydrogen, f_{H2}. For N_2-H_2 gas mixtures, $f_{HH} \approx f_{H2}$ and the deviation appears negligible for engineering applications. For CH_4-H_2 gas mixtures, $f_{HH} < f_{H2}$. The highest deviation is at f_{H2} = 12 MPa, where f_{HH} is calculated as low as about 9.4 MPa.

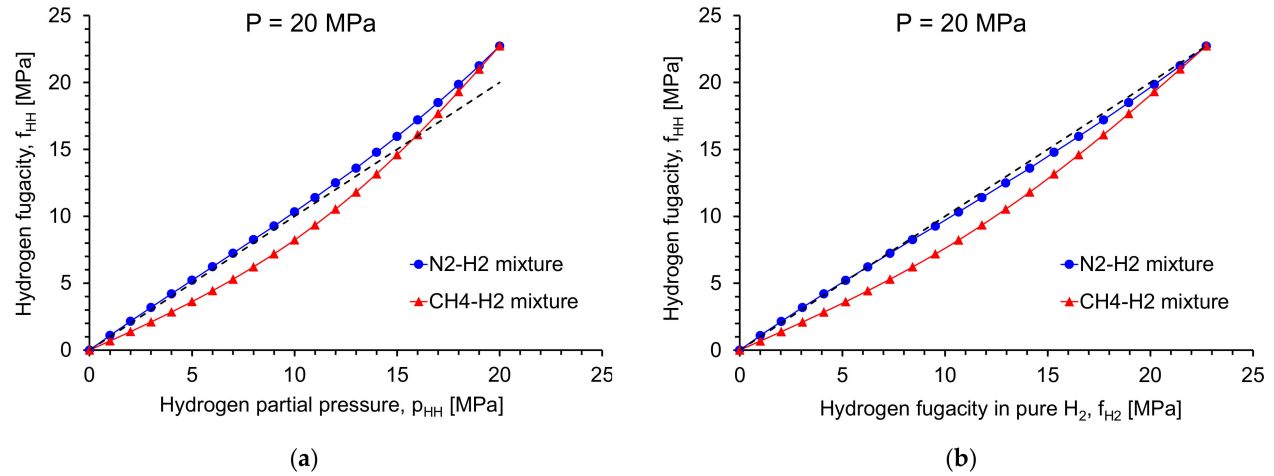

(**a**) (**b**)

Figure 4. Evolution of f_{HH} in N_2-H_2 and CH_4-H_2 gas mixtures at a total pressure of 20 MPa as a function of (**a**) p_{HH} and (**b**) fugacity of hydrogen in pure H_2 gas, f_{H2}. The dashed line represents the one-by-one ratio.

3. Compilation and Interpretation of Literature Results for Mechanical Properties as a Function of Hydrogen Fugacity

In the following, literature results from tests performed in pure hydrogen gas as well as in gas mixtures are plotted as a function of hydrogen fugacity *f*. The designation

"fugacity f" is used for both, hydrogen fugacity in pure H_2 and hydrogen fugacity in gas mixtures. The fugacities were calculated as described in chapter 0.

It is well known that the degradation of mechanical properties of steels tested in a gaseous hydrogen atmosphere increases with increasing hydrogen fugacity following a power law

$$HEI \sim mf^n \quad (8)$$

where *HEI* means any hydrogen embrittlement index, m is a factor and n is an exponent [2]. Typical hydrogen embrittlement indices use the ratio of the mechanical property measured in H_2 and in air, in percent. In this review, the relative reduction of area (RRA = RA_{H2}/RA_{air}) of tensile specimens (smooth and notched), the relative notched ultimate tensile strength (UTS_{H2}/UTS_{air}), the relative fracture toughness (K_{H2}/K_{air}), and the relative crack growth rate ($da/dN_{H2}/da/dN_{air}$) were calculated based on published experimental data. Using such indices, the degree of embrittlement increases as the index decreases except for the crack growth tests where the degree of embrittlement increases as the index increases because crack growth is accelerated in hydrogen compared to air. In the context of this study, literature results on the effect of pure gaseous hydrogen as well as gas mixtures upon the mechanical properties of API 5L X42, X52, X60, X70 and X80 grades were reviewed. The data discussed in the following focuses on X52, X70 and X80 grades where a comparatively large set of data is available to allow justified conclusions. The compilation of data from various sources revealed a large scatter so that the power law dependency described above is not always obvious. However, clear trends were observed and will be discussed despite the large scatter.

3.1. Tensile Tests

Tensile RRA of smooth specimens as a function of hydrogen fugacity for X70 and X80 steels is displayed in Figure 5a. It can be seen as a clear trend that RRA decreases with increasing hydrogen fugacity. A significant amount of results show RRA values around 100% up to a fugacity of about 1.2 MPa (dashed square in Figure 5a) whereas a single result reports a RRA value as low as about 75% at a fugacity as low as about 0.2 MPa [6] (arrow in Figure 5a). Since a large amount of data suggests negligible hydrogen effects at a low fugacity below 1.2 MPa, this review implies that tensile RRA of smooth specimens is a comparably insensitive *HEI* compared to other indices, as will be shown in the following.

Tensile RRA of notched specimens (range of stress intensity factors k_t between 2.4 and 6.3) as a function of hydrogen fugacity for X70 and X80 steels is depicted in Figure 5b. Notched RRA decreases rapidly from 98% at 0.1 MPa to about 80% at about 0.7 MPa (dashed square in Figure 5b). However, a single result reports a RRA value as low as about 45% at a fugacity as low as about 0.07 MPa [8] (arrow in Figure 5b). That is, it appears that tensile RRA of notched specimens is more sensitive to assess hydrogen effects in pipeline steels compared to tensile RRA of smooth specimens. This trend was not found for the corresponding values of the relative notched ultimate tensile strength, UTS (Figure 5c) where no significant degradation was reported up to a fugacity of 10.6 MPa.

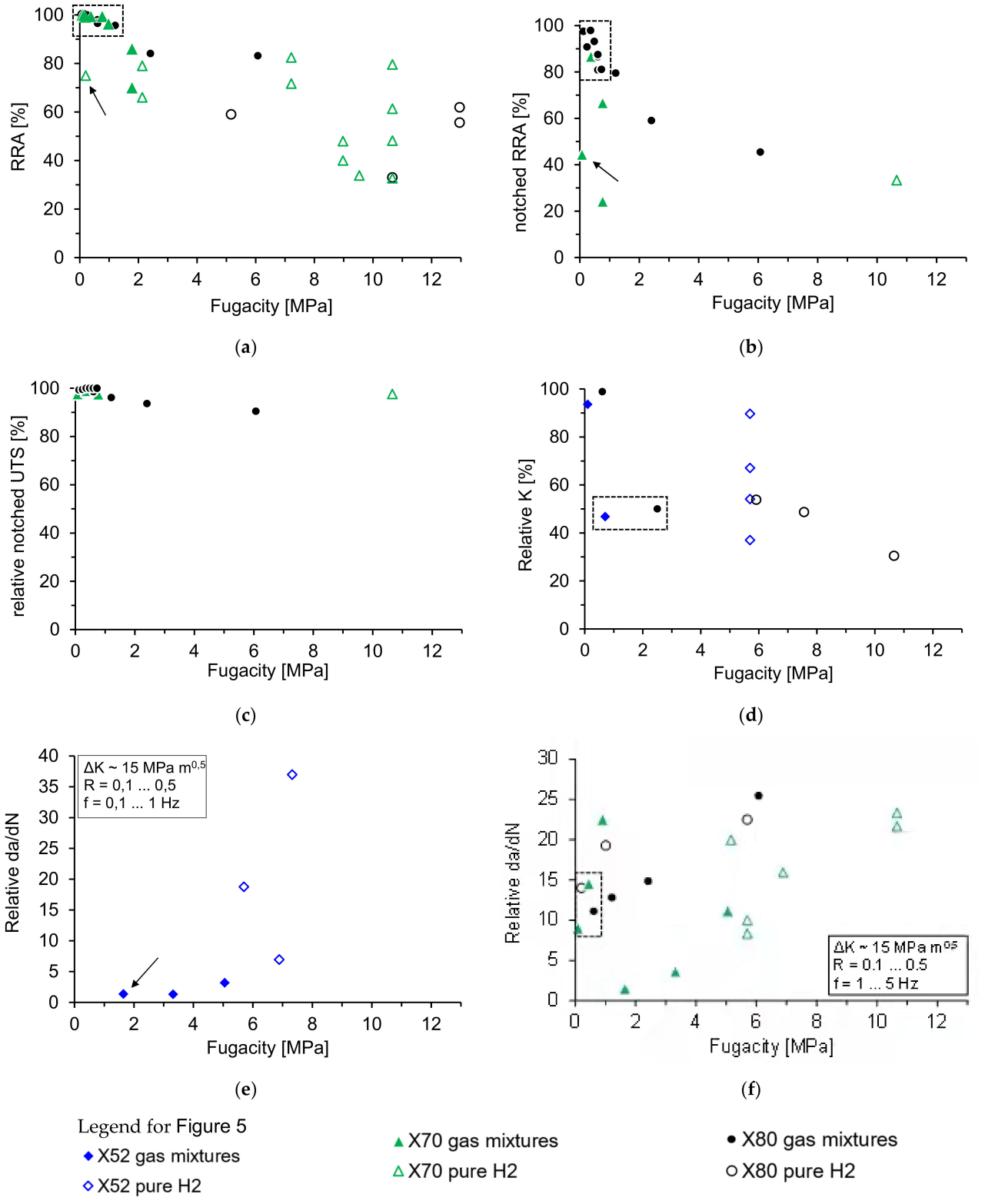

Figure 5. HEI as a function of hydrogen fugacity. (**a**) Tensile RRA of smooth specimens for X70 and X80 steels data from [6,8,9,26–36]. (**b**) Tensile RRA of notched specimens for X70 and X80 steels data from [7–9,37,38]. (**c**) Relative notched ultimate tensile strength for X70 and X80 steels data from [7–9,37,38]. (**d**) Relative fracture toughness (K) for X52 and X80 steels data from [39–45]. (**e**) Relative crack growth rate for X52 and (**f**) Relative crack growth rate for X70 as well as X80 steels data from [9,36,40,42,44,46–54].

3.2. Fracture Toughness Tests

The relative fracture toughness (K) as a function of hydrogen fugacity for X52 and X80 steels is plotted in Figure 5d. To increase the data set, elastic-plastic fracture toughness data obtained from J-integral tests were converted to K [39–41,44,45] using $K = (JE/(1-\nu^2))^{0.5}$. Also here, the relative fracture toughness decreases with increasing fugacity from nearly 100% at 0.6 MPa down to 30% at 10 MPa. Relative fracture toughness values between 45% and 50% are reported for low fugacities between 0.7 MPa and 2.0 MPa (dashed square in Figure 5d). From this review it appears that the sensitivity of fracture toughness results to hydrogen effects in pipeline steels is comparable to notched RRA results (Figure 5b) and significantly higher compared to notched UTS results (Figure 5c). The latter is surprising because a correlation between notched UTS and fracture toughness was reported for stress concentration factors k_t greater than 6 [55]. However, the stress concentration factors of the specimens tested in the referenced studies was less than 6, with one exception ($kt \approx 6.3$ [38]), which might be one reason for the lack of correlation between the two material properties.

3.3. Fatigue Crack Growth Tests

The relative crack growth rate as a function of hydrogen fugacity for X52, X70 and X80 steels is displayed in Figure 5e,f. For grade X52 an increase in crack growth rate by a factor of about 2 at a fugacity of 1.6 MPa was reported [36] (arrow in Figure 5e) whereas for X70/X80 grades an increase in crack growth rate by a factor of about 10 to 15 at a fugacity less than 0.5 MPa (dashed square in Figure 5f) was measured [9,44,53]. The results from grades X70 and X80 clearly indicate that the growth of an initial crack or flaw is greatly accelerated under the influence of gaseous hydrogen even at a hydrogen fugacity well below 1 MPa and it is worth to mention that no result was found which reports no increase in crack growth rate at a fugacity below 1 MPa.

3.4. General Comments

It was shown in the previous sections that all reviewed *HEI* follow the known trends as a function of hydrogen fugacity, i.e., all the *HEI* decrease with increasing fugacity except the relative crack growth rate which increases with increasing fugacity. Although this study only includes results where the test conditions were similar enough to allow a direct comparison of the results, the scatter of the reviewed data is high. Plausible reasons are the different chemical compositions and microstructures allowed within the respective steel specifications, slightly different test parameters (e.g., strain rate, frequency, R ratio) or test conditions (e.g., purity of the test gas especially oxygen residues) as well as differences in sample preparation. This clearly emphasizes the urgent necessity for the development of international test standards.

Furthermore, the results in gas mixtures (N_2-H_2, CH_4-H_2, NG-H_2) and in pure H_2 overlap, which indicates that hydrogen fugacity is the governing parameter for both, tests in pure hydrogen and tests in gas mixtures. It appears that the influence of the other gas (N_2, CH_4 or natural gas) upon hydrogen-surface interactions, i.e., transport of hydrogen to the crack tip, physical adsorption, dissociative chemical adsorption and absorption [2] is small and that their effect on the mechanical response is smaller than the scatter of the data. If this assumption is true, then test results obtained in gas mixtures and in pure hydrogen, both at the same fugacity, are equivalent. However, this conclusion must be verified since a study supporting this assumption by a direct comparison of results measured in gas mixtures and in pure hydrogen could not be found.

4. Conclusions

The aforementioned results allow the following conclusions:

- For materials testing purposes requiring a defined atmosphere, testing in CH_4-H_2 mixtures is preferred compared to N_2-H_2 mixtures to simulate the effect of H_2 additions to NG.

- The reviewed results imply no significant difference between tests in pure H_2 gas and tests in gas mixtures at the same hydrogen fugacity. This needs to be verified experimentally.
- Among the test methods reviewed here, fatigue crack growth testing is the most sensitive method to measure hydrogen effects in pipeline steels even at a very low fugacity (less than 0.5 MPa). Fracture toughness testing appears less sensitive followed by tensile testing, especially with smooth specimens.

Author Contributions: Conceptualization, T.M. and C.E.; methodology, T.M. and C.E.; formal analysis, T.M. and C.E.; investigation, T.M.; data curation, T.M. writing—original draft preparation, T.M. and C.E.; writing—review and editing, T.M., C.E., K.W. and F.S. All authors have read and agreed to the published version of the manuscript.

Funding: This research was financially supported by Fraunhofer through project "H_2 D–a hydrogen economy for Germany".

Institutional Review Board Statement: Not applicable.

Informed Consent Statement: Not applicable.

Data Availability Statement: Not applicable.

Acknowledgments: The authors would like to thank Christopher San Marchi from Sandia National Laboratories, Livermore, CA, USA for very helpful discussions.

Conflicts of Interest: The authors declare no conflict of interest.

References

1. Cerniauskas, S.; Junco, A.J.C.; Grube, T.; Robinius, M.; Stolten, D. Options of natural gas pipeline reassignment for hydrogen: Cost assessment for a Germany case study. *Int. J. Hydrog. Energy* **2020**, *45*, 12095–12107. [CrossRef]
2. Michler, T.; Wackermann, K.; Schweizer, F. Review and Assessment of the Effect of Hydrogen Gas Pressure on the Embrittlement of Steels in Gaseous Hydrogen Environment. *Metals* **2021**, *11*, 637. [CrossRef]
3. Marchi, C.S.; Somerday, B.P.; Larson, R.S.; Rice, S.F. Solubility of hydrogen and its isotopes in metals from mixed gases. *J. Nucl. Mater.* **2008**, *372*, 421–425. [CrossRef]
4. Somerday, B.P.; Sofronis, P.; Nibur, K.A.; Marchi, C.S.; Kirchheim, R. Elucidating the variables affecting accelerated fatigue crack growth of steels in hydrogen gas with low oxygen concentrations. *Acta Mater.* **2013**, *61*, 6153–6170. [CrossRef]
5. Michler, T.; Boitsov, I.E.; Malkov, I.L.; Yukhimchuk, A.A.; Naumann, J. Assessing the effect of low oxygen concentrations in gaseous hydrogen embrittlement of DIN 1.4301 and 1.1200 steels at high gas pressures. *Corros. Sci.* **2012**, *65*, 169–177. [CrossRef]
6. Ez-Zaki, H.; Christien, F.; Bosch, C.; Briottet, L.; Bertin, M.; Levasseur, O.; Leriverain, A. Effect of hydrogen content in natural gas blend on the mechanical properties of a L485-MB low-alloyed steel. In Proceedings of the ASME 2020 Pressure Vessels & Piping Conference, Viral Conference, 19–24 July 2020; ASME Press: Minneapolis, MN, USA, 2020; p. PVP2020–21228. [CrossRef]
7. Shang, J.; Zheng, J.; Hua, Z.; Li, Y.; Gu, C.; Cui, T.; Meng, B. Effects of stress concentration on the mechanical properties of X70 in high-pressure hydrogen-containing gas mixtures. *Int. J. Hydrog. Energy* **2020**, *45*, 28204–28215. [CrossRef]
8. Baek, U.; Nahm, S.; Lee, H.; Lee, Y. Mechanical Properties of X70 Steel in Gaseous Hydrogen. In Proceedings of the International Hydrogen Conference (IHC 2012): Hydrogen-Materials Interactions, Moran, WY, USA, 9–12 September 2012; pp. 219–226. [CrossRef]
9. Meng, B.; Gu, C.; Zhang, L.; Zhou, C.; Li, X.; Zhao, Y.; Zheng, J.; Chen, X.; Han, Y. Hydrogen effects on X80 pipeline steel in high-pressure natural gas/hydrogen mixtures. *Int. J. Hydrog. Energy* **2017**, *42*, 7404–7412. [CrossRef]
10. Marchi, C.S.; Somerday, B.P.; Robinson, S.L. Permeability, solubility and diffusivity of hydrogen isotopes in stainless steels at high gas pressures. *Int. J. Hydrog. Energy* **2007**, *32*, 100–116. [CrossRef]
11. Sugimoto, H.; Fukai, Y. Solubility of hydrogen in metals under high hydrogen pressures: Thermodynamical calculations. *Acta Met. Mater.* **1992**, *40*, 2327–2336. [CrossRef]
12. Marchi, C.S.; Somerday, B.P. Thermodynamics of Gaseous Hydrogen and Hydrogen Transport in Metals. In Proceedings of the MRS Spring 2008 Meeting, Session HH: "The Hydrogen Economy", San Francisco, CA, USA, 24–28 March 2008; pp. 1–12.
13. Chenoweth, D.R. *Gas-Transfer Analysis. Section H-Real Gas Results Via the Van der Waals Equation of State and Virial Expansion Extension of its Limiting Abel-Noble Form*; U.S. Department of Energy, Office of Scientific and Technical Information: Washington, DC, USA, 1983; p. 87.
14. Chenoweth, D.R.; Paolucci, S. Compressible flow of a two-phase fluid between finite vessels-II. *Int. J. Multiph. Flow.* **1992**, *18*, 669–689. [CrossRef]
15. Michels, A.; Wouters, H.; de Boer, J. Isotherms of nitrogen between 0° and 150° and at pressures from 20 to 80 atm. *Physica* **1934**, *1*, 587–594. [CrossRef]

16. Michels, A.; Lunbeck, R.J.; Wolkers, G.J. Thermodynamical properties of nitrogen as functions of density and temperature between −125° and +150 °C and densities up to 760 Amagat. *Physica* **1951**, *17*, 801–816. [CrossRef]
17. Isotherms of hydrogen, of nitrogen, and of hydrogen-nitrogen mixtures, at 0° and 20 °C, up to a pressure of 200 atmospheres. *Proc. R. Soc. Lond. Ser. A* **1926**, *111*, 552–576. [CrossRef]
18. Trappeniers, N.J.; Wassenaar, T.; Abels, J.C. Isotherms and thermodynamic properties of methane at temperatures between 0° and 150°C and at densities up to 570 amagat. *Phys. A* **1979**, *98*, 289–297. [CrossRef]
19. Kvalnes, H.M.; Gaddy, V.L. The compressibility isotherms of methane at pressures to 1000 atmospheres and at temperatures from −70 to 200°. *J. Am. Chem. Soc.* **1931**, *53*, 394–399. [CrossRef]
20. Schley, P.; Jaeschke, M.; Küchenmeister, C.; Vogel, E. Viscosity measurements and predictions for natural gas. *Int. J. Thermophys.* **2004**, *25*, 1623–1652. [CrossRef]
21. Mihara, S.; Sagara, H.; Arai, Y.; Saito, S. The Compressibility Factors of Hydrogen Methane, Hydrogen Ethane and Hydrogen Propane Gaseous Mixtures. *J. Chem. Eng.* **1977**, *10*, 395–399. [CrossRef]
22. Azizi, N.; Behbahani, R.; Isazadeh, M.A. An efficient correlation for calculating compressibility factor of natural gases. *J. Nat. Gas Chem.* **2010**, *19*, 642–645. [CrossRef]
23. Čapla, L.; Buryan, P.; Jedelský, J.; Rottner, M.; Linek, J. Isothermal pVT measurements on gas hydrocarbon mixtures using a vibrating-tube apparatus. *J. Chem. Thermodyn.* **2002**, *34*, 657–667. [CrossRef]
24. Zhou, J.; Patil, P.; Ejaz, S.; Atilhan, M.; Holste, J.C.; Hall, K.R. (p, Vm, T) and phase equilibrium measurements for a natural gas-like mixture using an automated isochoric apparatus. *J. Chem. Thermodyn.* **2006**, *38*, 1489–1494. [CrossRef]
25. Langelandsvik, L.I.; Solvang, S.; Rousselet, M.; Metaxa, I.N.; Assael, M.J. Dynamic viscosity measurements of three natural gas mixtures-comparison against prediction models. *Int. J. Thermophys.* **2007**, *28*, 1120–1130. [CrossRef]
26. Duncan, A.; Lam, P.-S.; Adams, T. Tensile testing of carbon steel in high pressure hydrogen. In Proceedings of the ASME 2007 Pressure Vessels and Piping Conference, San Antonio, TX, USA, 22–26 July 2007; p. PVP2007–PVP26736.
27. Kussmaul, K.; Deimel, P.; Sattler, E. Tensile properties of the steel X70TM in high pressure hydrogen gas with admixtures of oxygen at different strain rates. In Proceedings of the 10th World Energy Conference Cocoa Hydrogen Energy Progress X, Boca Beach, FL, USA, 20–24 June 1994; pp. 285–293.
28. Michler, T.; Naumann, J. Microstructural aspects upon hydrogen environment embrittlement of various bcc steels. *Int. J. Hydrog. Energy* **2010**, *35*, 821–832. [CrossRef]
29. Bae, D.S.; Sung, C.E.; Bang, H.J.; Lee, S.P.; Lee, J.K.; Son, I.S.; Cho, Y.R.; Baek, U.B.; Nahm, S.H. Effect of highly pressurized hydrogen gas charging on the hydrogen embrittlement of API X70 steel. *Met. Mater. Int.* **2014**, *20*, 653–658. [CrossRef]
30. Hejazi, D.; Calka, A.; Dunne, D.; Pereloma, E. Effect of gaseous hydrogen charging on the tensile properties of standard and medium Mn X70 pipeline steels. *Mater. Sci. Technol.* **2016**, *32*, 675–683. [CrossRef]
31. Baek, U.B.; Lee, H.M.; Baek, S.W.; Nahm, S.H. Hydrogen Embrittlement for X-70 Pipeline Steel in High Pressure Hydrogen Gas. In Proceedings of the ASME 2015 Pressure Vessels and Piping Conference, Boston, MA, USA, 19–23 July 2015; ASME Press: Boston, MA, USA, 2015; p. PVP2015–PVP45475. [CrossRef]
32. Zhou, D.; Li, T.; Huang, D.; Wu, Y.; Huang, Z.; Xiao, W.; Wang, Q.; Wang, X. The experiment study to assess the impact of hydrogen blended natural gas on the tensile properties and damage mechanism of X80 pipeline steel. *Int. J. Hydrog. Energy* **2021**, *46*, 7402–7414. [CrossRef]
33. Moro, I.; Briottet, L.; Lemoine, P.; Andrieu, E.; Blanc, C.; Odemer, G. Hydrogen embrittlement susceptibility of a high strength steel X80. *Mater. Sci. Eng. A* **2010**, *527*, 7252–7260. [CrossRef]
34. Zhang, T.; Zhao, W.; Zhao, Y.; Ouyang, K.; Deng, Q.; Wang, Y.; Jiang, W. Effects of surface oxide films on hydrogen permeation and susceptibility to embrittlement of X80 steel under hydrogen atmosphere. *Int. J. Hydrog. Energy* **2018**, *43*, 3353–3365. [CrossRef]
35. Batisse, R.; Cuni, A.; Wastiaux, S.; Briottet, L.; Lemoine, P.; de Dinechin, G.; Chagnot, C.; Castilan, F.; Klosek, V.; Langlois, P.; et al. Investigation of X80-steel grade for hydrogen gas transmission pipelines. In Proceedings of the 2008 International Gas Research Conference, Paris, France, 8–10 October 2008; Gas Technology Institute: Paris, France, 2008; pp. 1572–1588.
36. Van Wortel, H.; Gomes, M.; Demofoni, G.; Capelle, J.; Alliat, J.; Chatzidouros, E. Final report "Preparing for the hydrogen economy by using the existing natural gas system as a catalyst (NATURALHY) WP3.2: Transmission pipelines, 2009" Funded by the EU within the 6th framework programme.
37. Zhou, Z.; Zhang, K.; Hong, Y.; Zhu, H.; Zhang, W.; He, Y.; Zhou, C.; Zheng, J.; Zhang, L. The dependence of hydrogen embrittlement on hydrogen transport in selective laser melted 304L stainless steel. *Int. J. Hydrog. Energy* **2021**, *46*, 16153–16163. [CrossRef]
38. Shi, H.; Xing, Y.; Wang, X. Influence law of hydrogen content in coal gas system on hydrogen embrittlement sensitivity of X80 pipeline steel. *Corros. Prot.* **2018**, *39*, 336–339.
39. Shang, J.; Wang, J.Z.; Chen, W.F.; Wei, H.T.; Zheng, J.Y.; Hua, Z.L.; Zhang, L.; Gu, C.H. Different effects of pure hydrogen vs. hydrogen/natural gas mixture on fracture toughness degradation of two carbon steels. *Mater. Lett.* **2021**, *296*, 129924. [CrossRef]
40. Marchi, C.S.; Somerday, B.P.; Nibur, K.A.; Stalheim, D.G.; Boggess, T.; Jansto, S. Fracture and fatigue of commercial grade API pipeline steels in gaseous hydroge. In Proceedings of the ASME 2010 Pressure Vessels and Piping Division Conference (PVP 2010), Washington, DC, USA, 18–22 July 2010; p. PVP2010–2PVP5825.
41. Cialone, H.J.; Holbrook, J.H. Sensitivity of Steels to Degradation in Gaseous Hydrogen. In *ASTM STP 962*; Raymond, E.L., Ed.; ASTM International: Philadelphia, PA, USA, 1988; pp. 134–152.

42. Ronevich, J.A.; Marchi, C.S. Materials compatibility concerns for hydrogen blended into natural gas. In Proceedings of the ASME 2021 Pressure Vessels and Piping Conference (PVP2021), Virtual Online Conference, 12–16 July 2021; ASME Press: New York, NY, USA, 2021; p. PVP2021–PVP62045.
43. Stalheim, D.; Jansto, S.G.; Boggess, T.; Ningileri, S.; Bromley, D. Microstructure and mechanical property performance evaluation of commercial grade API pipeline steels in high pressure gaseous hydrogen. In Proceedings of the 2012 International Hydrogen Conference Hydrogen-Materials Interactions, Moran, WY, USA, 9–12 September 2012; Somerday, B.P., Sofronis, P., Eds.; ASME Press: Jackson Lake Lodge, WY, USA, 2012; pp. 209–218.
44. An, T.; Zhang, S.; Feng, M.; Luo, B.; Zheng, S.; Chen, L.; Zhang, L. Synergistic action of hydrogen gas and weld defects on fracture toughness of X80 pipeline steel. *Int. J. Fatigue* **2019**, *120*, 23–32. [CrossRef]
45. Zhang, S.; Li, J.; An, T.; Zheng, S.; Yang, K.; Lv, L.; Xie, C.; Chen, L.; Zhang, L. Investigating the influence mechanism of hydrogen partial pressure on fracture toughness and fatigue life by in-situ hydrogen permeation. *Int. J. Hydrog. Energy* **2021**, *46*, 20621–20629. [CrossRef]
46. Drexler, E.S.; Slifka, A.J.; Amaro, R.L.; Sowards, J.W.; Connolly, M.J.; Martin, M.L.; Lauria, D.S. Fatigue Testing of Pipeline Welds and Heat-Affected Zones in Pressurized Hydrogen Gas. *J. Res. Natl. Inst. Stand. Technol.* **2019**, *124*, 124008. [CrossRef]
47. Drexler, E.S.; Slifka, A.J.; Amaro, R.L.; Barbosa, N.; Lauria, D.S.; Hayden, L.E.; Stalheim, D.G. Fatigue crack growth rates of API X70 pipeline steel in a pressurized hydrogen gas environment. *Fatigue Fract. Eng. Mater. Struct.* **2014**, *37*, 517–525. [CrossRef]
48. Slifka, A.J.; Drexler, E.S.; Stalheim, D.G.; Amaro, R.L.; Lauria, D.S.; Stevenson, A.E.; Hayden, L.E. The effect of microstructure on the hydrogen-assisted fatigue of pipeline steels. In Proceedings of the ASME 2013 Pressure Vessels and Piping Conference (PVP2013), Paris, France, 14–18 July 2013; ASME Press: Paris, France, 2013; p. PVP2013–PVP97217.
49. Drexler, E.S.; Amaro, R.L.; Slifka, A.J.; Bradley, P.E.; Lauria, D.S. Operating Hydrogen Gas Transmission Pipelines at Pressures Above 21 MPa. *J. Press. Vessel Technol.* **2018**, *140*, 61702. [CrossRef]
50. Baek, U.B.; Nahm, S.H.; Kim, W.S.; Ronevich, J.A.; Marchi, C.S. Compatibility and suitability of existing steel pipeline for transport of hydrogen-natural gas blends. In Proceedings of the International Conference on Hydrogen Safety, Hamburg, Germany, 11–13 September 2017.
51. Slifka, A.J.; Drexler, E.S.; Nanninga, N.E.; Levy, Y.S.; McColskey, J.D.; Amaro, R.L.; Stevenson, A.E. Fatigue crack growth of two pipeline steels in a pressurized hydrogen environment. *Corros. Sci.* **2014**, *78*, 313–321. [CrossRef]
52. Ronevich, J.A.; Somerday, B.P.; Feng, Z. Hydrogen accelerated fatigue crack growth of friction stir welded X52 steel pipe. *Int. J. Hydrog. Energy* **2017**, *42*, 4259–4268. [CrossRef]
53. Chandra, A.; Thodla, R.; Prewitt, T.J.; Matthews, W.; Sosa, S. Fatigue Crack Growth Study of X70 Line Pipe Steel in Hydrogen Containing Natural Gas Blends. In Proceedings of the ASME 2021 Pressure Vessels and Piping Conference (PVP2021), Virtual Conference, 12–16 July 2021; ASME Press: New York, NY, USA, 2021; p. PVP2021–PVP61821.
54. Engel, V.C.; Marewski, U.; Schnotz, G.; Silcher, H.; Steiner, M.; Zickler, S. Bruchmechanische Prüfungen von Werkstoffen für Gasleitungen zur Bewertung der Wasserstofftauglichkeit: Erste Ergebnisse (In German), 3R Fachzeitschrift Für Sichere Und Effiziente Rohrleitungssysteme. *Pipelintechnik* **2020**, *10–11*, 34–41.
55. Lee, J.A. Rapid and low cost method to determine the plane strain fracture toughness (K1C) in hydrogen. In Proceedings of the 2012 International Hydrogen Conference Hydrogen-Materials Interactions, Moran, WY, USA, 9–12 September 2012; Sofronis, P., Ed.; ASME Press: Jackson Lake Lodge, WY, USA, 2012; pp. 461–470.